Steric and Electronic Effect of Cp-Substituents on the Structure of the Ruthenocene Based Pincer Palladium Borohydrides

**Sergey V. Safronov *, Elena S. Osipova, Yulia V. Nelyubina, Oleg A. Filippov,
Irina G. Barakovskaya, Natalia V. Belkova * and Elena S. Shubina**

A. N. Nesmeyanov Institute of Organoelement Compounds, Russian Academy of Sciences, 28 Vavilova Str.,
119991 Moscow, Russia; aosipova92@gmail.com (E.S.O.); unelya@xrlab.ineos.ac.ru (Y.V.N.);
h-bond@ineos.ac.ru (O.A.F.); analyst@ineos.ac.ru (I.G.B.); shu@ineos.ac.ru (E.S.S.)

* Correspondence: sergiosfr-hcc@mail.ru (S.V.S.); nataliabelk@ineos.ac.ru (N.V.B.)

Abstract: Ruthenocene-based PCP^{tBu} pincer ligands were used to synthesize novel pincer palladium chloride $Rc^F[PCP^{tBu}]PdCl$ (**2a**) and two novel palladium tetrahydroborates $Rc^F[PCP^{tBu}]Pd(BH_4)$ (**3a**) and $Rc^*[PCP^{tBu}]Pd(BH_4)$ (**3b**), where $Rc^F[PCP^{tBu}] = \kappa^3\text{-}\{2,5\text{-}(tBu_2PCH_2)_2\text{-}C_5H_2\}Ru(Cp^F)$ ($Cp^F = C_5Me_4CF_3$), and $Rc^*[PCP^{tBu}] = \kappa^3\text{-}\{2,5\text{-}(tBu_2PCH_2)_2C_5H_2\}Ru(Cp^*)$ ($Cp^* = C_5Me_5$). These coordination compounds were characterized by X-ray, NMR and FTIR techniques. Analysis of the X-ray data shows that an increase of the steric bulk of non-metalated cyclopentadienyl ring in **3a** and **3b** relative to non-substituted $Rc[PCP^{tBu}]Pd(BH_4)$ analogue (**3c**; where $Rc[PCP^{tBu}] = \kappa^3\text{-}\{2,5\text{-}(tBu_2PCH_2)_2C_5H_2\}Ru(Cp)$, $Cp = C_5H_5$) pushes palladium atom from the middle plane of the metalated Cp ring in the direction opposite to the ruthenium atom. This displacement increases in the order **3c** < **3b** < **3a** following the order of the Cp-ring steric volume increase. The analysis of both X-ray and IR data suggests that BH_4 ligand in both palladium tetrahydroborates **3a** and **3b** has the mixed coordination mode $\eta^{1,2}$. The strength of the BH_4 bond with palladium atom increases in the order $Rc[PCP^{tBu}]Pd(BH_4) < Rc^*[PCP^{tBu}]Pd(BH_4) < Rc^F[PCP^{tBu}]Pd(BH_4)$ that appears to be affected by both steric and electronic properties of the ruthenocene moiety.

Keywords: pincer; ligand; palladium; ruthenocene; tetrahydroborate

1. Introduction

The chemistry of transition metal complexes with pincer-type ligands has been actively studied since the 1970s [1]. Such complexes feature a unique balance of stability and reactivity, which can be controlled by the systematic modification of ligands, and thus a huge potential for the use in organic synthesis and catalysis [2–12]. A continuous search for more active and selective catalysts, including asymmetric ones, has led to the appearance of new bimetallic complexes of transition metals with pincer ligands of sandwich-type containing cyclometalated five- [13–22] (**A**) and six-membered [23–30] (**B**) aromatic rings (Scheme 1).
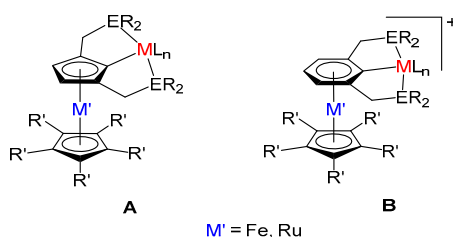
Scheme 1. General structures of metallocene-based pincer complexes. $ER_2 = PR_2$, NR_2 where R = alkyl, aryl; R′ = H, CH_3, CF_3, etc.

The presence of a transition metal in the sandwich moiety allows varying the charge of the bimetallic complex and significantly affects the electrochemical characteristics of the chelated η^1-metal center [23]. For example, in comparison with neutral precursors, the presence of a positive charge in bimetallic ruthenium–palladium complexes leads to a decrease in the electron density on the chelated palladium atom and contributes to an increase in its catalytic activity in Suzuki cross-coupling reactions [19,24,26]. It can be assumed that the introduction of electron-withdrawing groups into the sandwich core of the bimetallic complex can favorably affect the catalytic properties of the chelated metal atom. On the other hand, it is well known that in addition to the electronic factor, the catalytic activity of metal complexes is strongly affected by steric factors determining the spatial availability of the metal center for the substrate [8,15,16,31]. In the case of bimetallic PCP complexes of sandwich-type, the steric accessibility of the chelated metal atom is determined not only by the volume of organic groups R at the phosphorus donor atoms and the P-M-P angle but also by the presence of substituents in the non-metalated ring [17,23,25]. Thus, the presence of five methyl groups in the cyclopentadienyl ligand significantly increases its steric volume and donor ability in comparison with the unsubstituted Cp ring (Cp = η^5-C_5H_5). Replacing one of the methyl groups in the Cp* ligand (Cp* = η^5-C_5Me_5) with CF_3 group ($Cp^F = C_5Me_4CF_3$) slightly increases the volume of the five-membered ring, but keeps the electronic effect of the ligand at the level of unsubstituted cyclopentadienyl [32–35].

An interesting feature of palladium chloride complexes based on ferrocene and ruthenocene is their ability to react with $NaBH_4$ to form the corresponding tetrahydroborate complexes $Fc[PCP^{tBu}]Pd(BH_4)$ and $Rc[PCP^{tBu}]Pd(BH_4)$. (where $Fc[PCP^{tBu}]$ and $Rc[PCP^{tBu}]$ = κ^3-{2,5-($^tBu_2PCH_2)_2C_5H_2$}M(Cp), M = Fe, Ru) [15,36]. $Rc[PCP^{tBu}]Pd(BH_4)$ complex, which we have recently studied [36], proved to be a useful starting compound for the production of highly reactive palladium hydride $Rc[PCP^{tBu}]PdH$. However, despite a high potential of complexes of this type, the sterically loaded palladium pincer complexes remain almost unexplored. In this work, we report on the synthesis of two new palladium borohydride pincer complexes based on substituted ruthenocenes. The use of Cp* and Cp^F ligands and comparison with the non-substituted Cp analogues allows accessing the steric and electronic effects of sandwich moiety on the properties of PCP^{tBu} chelated palladium.

2. Results and Discussion

2.1. Synthesis

1,3-disubstituted ruthenocene bisphosphine with a Cp^F ligand in the metallocene core {1,3-($^tBu_2PCH_2)_2C_5H_2$}Ru(Cp^F) (**1**) was synthesized by phosphination of the corresponding diol {1,3-(HOCH$_2)_2C_5H_2$}Ru(Cp^F) in acetic acid according to the previously published procedure [37]. The cyclometalation of **1** with $PdCl_2(PhCN)_2$ in 2-methoxyethanol under reflux for 3 h (Scheme 2) yields the new palladium complex $Rc^F[PCP^{tBu}]PdCl$ (**2a**) (where $Rc^F[PCP^{tBu}]$ = κ^3-{2,5-($tBu_2PCH_2)_2C_5H_2$}Ru($C_5Me_4CF_3$)).
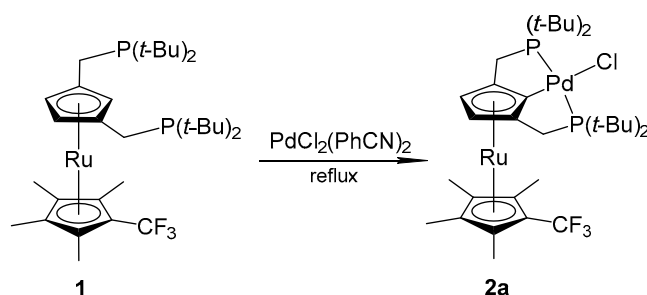
Scheme 2. Cyclopalladation reaction.

As the reaction proceeds, a finely dispersed, unidentified, bright yellow precipitate and impurities are formed that significantly complicate the subsequent isolation of the target cyclometalation product. To facilitate the isolation of **2a**, two equivalents of triethylamine were introduced into the reaction mixture after 3 h of reflux, which was continued for another 2 h. This approach led to the formation of a significant amount of palladium black, however, it allowed simplifying the purification procedure and gave the product with 31% yield. Note that the analogues palladium complex based on pentamethylruthenocene Rc*[PCP^{tBu}]PdCl (**2b**) (where Rc*[PCP^{tBu}] = κ^3-{2,5-(^{t}Bu$_2$PCH$_2$)$_2$C$_5$H$_2$}Ru(C$_5$Me$_5$)) was previously obtained under similar conditions with 30% yield. Apparently, the serious steric hindrance in the bisphosphine molecule created by the presence of five substituents in the cyclopentadienyl ring and tert-butyl groups at the donor phosphorus atoms hampers the cyclometalation reaction. For comparison, [PCP^{tBu}] complexes of palladium based on ferrocene, ruthenocene, and benzene can be obtained under comparable conditions with much higher yields [1,15,17]. It has been reported that in the preparation of benzene-based [POCOP^{tBu}] palladium complex the replacement of the most frequently used PdCl$_2$(PhCN)$_2$ as a cyclometalating agent with palladium(II) chloride leads to an increase in the yield of the reaction product from 31 to 80% [38]. Unfortunately, the use of PdCl$_2$ as a cyclometalation reagent in the reaction with Rc^F[PCP^{tBu}] (**1**) led to the formation of complex **2a** only in trace amounts. Compound **2a** is a pale yellow, air-stable powder. It was characterized by multinuclear NMR spectroscopy, and its purity was confirmed by elemental analysis.

The ^{31}P{^{1}H} and ^{19}F NMR spectra of complex **2a** contain a single signal from two equivalent phosphorus nuclei and three equivalent fluorine nuclei at δ 82.07 ppm and −52.74 ppm, respectively. In the ^{1}H NMR, the proton signal of the metallated cyclopentadienyl ring is observed as a singlet at 4.22 ppm (2H). The signal of the six protons of two methyl groups located at the 2′,5′ positions of the Cp^F ligand appears as a broadened multiplet at δ 1.89 ppm and the proton signals of two other methyl groups of the same ligand as a singlet at δ 1.77 ppm. Geminal methylene protons of CH$_2$P^{t}Bu$_2$ groups are not equivalent and appear as doublets of virtual triplets at δ 2.45 and 2.51 ppm. Resonances of methyl protons of nonequivalent tert-butyl groups are observed in the form of two virtual triplets at δ 1.33 ppm and 1.47 ppm in accordance with the expected structure.

The reaction of Rc^F[PCP^{tBu}]PdCl (**2a**) and Rc*[PCP^{tBu}]PdCl (**2b**) with an excess of NaBH$_4$ in refluxing ethanol leads to the formation of the corresponding tetrahydroborate complexes Rc^F[PCP^{tBu}]Pd(BH$_4$) (**3a**) and Rc*[PCP^{tBu}]Pd(BH$_4$) (**3b**) (Scheme 3).

The complete conversion of the starting chlorides **2** into borohydrides **3** can be reached in 8 h, adding extra NaBH$_4$ to the reaction mixture every hour. Monitoring of the formation of complex **3b** using NMR spectroscopy showed that after 3 h of reflux the ratio of the reaction product to the starting compound is approximately 3:1. The formation of palladium hydride complexes was not observed. For comparison, the pincer chloropalladium complexes based on ferrocene Fc[PCP^{tBu}]PdCl [15] and ruthenocene Rc[PCP^{tBu}]PdCl [36] are completely converted to the corresponding tetrahydroborates in 2 h. Complexes **3a** and **3b** were isolated in analytically pure form with 90% and 93% yield, respectively, as bright yellow crystalline powders. They are stable at room temperature in the solid state but are sensitive to air and thermally unstable in solution. In chloroform, **3a** and **3b** rapidly transform

into the chloropalladium precursors **2a** and **2b**. In general, sterically loaded borohydride complexes **3a** and **3b** are less stable than the previously obtained ruthenocene analogue Rc[PCP^{tBu}]Pd(BH$_4$) (**3c**) [36]. Compounds **3a** and **3b** were fully characterized by NMR, IR, and elemental analysis. The presence of BH$_4$ ligand coordinated to the palladium atom is confirmed by ^{1}H and ^{11}B NMR spectroscopy. The BH$_4$ protons appear in the ^{1}H NMR spectrum as a strongly broadened multiplet at δ_H 0.13 and 0.21 ppm for **3a** and **3b** in C$_6$D$_6$, respectively. ^{11}B{^{1}H} NMR spectra exhibit broadened signals at δ −34.54 and −34.73, respectively. The broadening of the BH$_4$ group signals in the ^{1}H NMR spectra indicates a rapid averaging in solution of hydrogen atoms bound to boron. The ^{31}P{^{1}H} NMR spectra of complexes **3a** and **3b** exhibit singlets at δ_P 87.44 and 87.07, respectively, indicating the equivalence of two phosphorus nuclei.

2a: R = CF$_3$
2b: R = Me

3a: R = CF$_3$
3b: R = Me
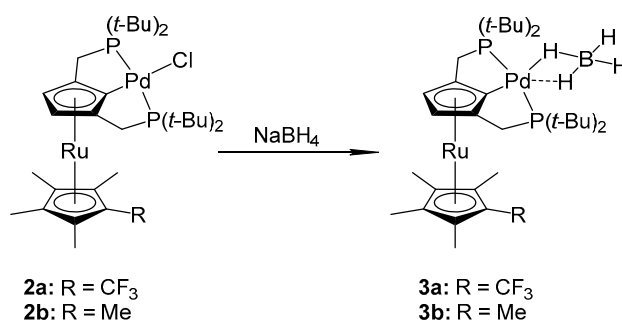
Scheme 3. Synthesis of borohydrides **3a** and **3b**.

2.2. X-Ray Diffraction Study

The structures of complexes **3a** and **3b** are very similar as confirmed by single-crystal XRD analysis (Figures 1 and 2). They feature palladium atoms in a distorted square-planar environment with an angle P(1)-Pd(1)-P(2) equal to 155.67(2) and 158.87(5)°, respectively. Palladium atom deviates from the middle plane of the metalated Cp ring in the direction opposite to the ruthenium atom by 0.541(3) and 0.489(9) Å, respectively. For comparison, in the Rc[PCP^{tBu}]Pd(BH$_4$) complex (**3c**) the distance between the palladium atom and the plane of the Cp ring is 0.322 Å [36]. In both structures, the phosphorus atoms P(1) and P(2) rise above the Cp ring plane to different degrees: by 0.888(3) and 0.591(3) Å in case of **3a**; 0.708(10) and 0.501(11) Å in case of **3b**. The presence of five organic substituents in the non-metalated Cp ring makes the cyclopentadienyl rings noticeably non-coplanar. The angle between the planes of the cyclopentadienyl rings is 8.75(8) and 9.9(2)° in **3a** and **3b**, respectively. Similar values of this angle are reported for palladium chloride complex Rc*[PCP^{tBu}]PdCl (**2b**) [17].

It is known that the BH$_4$ anion can be coordinated to a transition metal atom in a monodentate (η^1), bidentate (η^2), or tridentate (η^3) fashion [39]. According to our X-ray diffraction data, in complexes **3a** and **3b** the BH$_4$ group is located in the *syn* position to the metallocene core relative to the Pd-C(1) bond line. The distance Pd-H(1) is 1.86(2) and 1.82(5) Å, respectively. These values significantly exceed the Pd-H bond length (1.53–1.75 Å) in the known palladium hydride pincer complexes [38,40,41] and are comparable to the values found for the ruthenocene-based complex Rc[PCP^{tBu}]Pd(BH$_4$) **3c** (1.87(2) Å) [36]. The distance of the Pd atom to the second nearest hydrogen atom H(2) in structures **3a**, **3b** is 2.46(2) and 2.34(6) Å, respectively (for comparison, d(Pd-H(2)) = 2.54(3) Å in **3c** [36]) that is below the sum of Pd-H van der Waals radii. The difference between the distances Pd-H(1) and Pd-H(2) in **3a** and **3b** Δd(Pd···H) = 0.60(2) and 0.52(5) Å is slightly lower than in **3c**. These values are comparable to Δd(Pd···H) in the previously described palladium borohydride complexes and fall in the reported range 0.2–0.67 Å [15,36,42,43]. An analysis of the above data votes for the monodentate η^1 type of BH$_4$ binding to palladium atom with more pronounced secondary Pd···H interaction relative to **3c**. However, according to our DFT calculations for complex **3c** the elongated Pd-H(2) contact makes an important additional contribution to the total binding of the BH$_4$ fragment to the palladium atom [36]. We believe

that in complexes **3a** and **3b**, featuring even shorter Pd-H(2) distances, the coordination of the BH$_4$ ligand to the palladium atom can be described as the intermediate η^{1,2} type similar to **3c**.
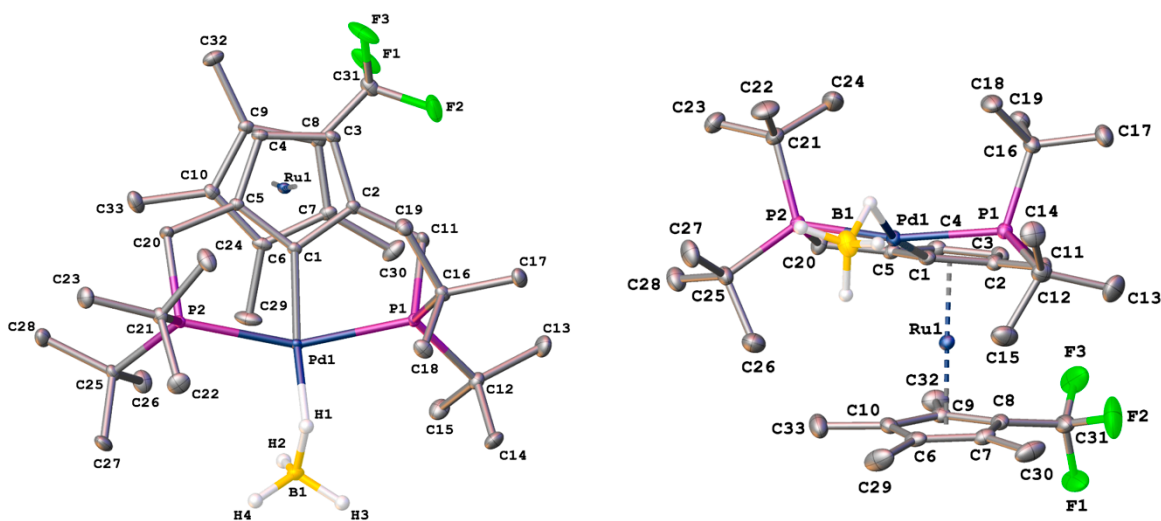

Figure 1. Two views of the compound **3a** with thermal ellipsoids at 50% probability level. Selected bond lengths (Å) and angles (°): Pd(1)–C(1) 1.9844(18), Pd(1)–P(1) 2.3447(5), Pd(1)–P(2) 2.3679(5), Pd(1)···B(1) 2.531(2), Pd(1)–H(1) 1.86(2), Pd(1)···H(2) 2.46(2); C(1)–Pd(1)–H(1) 167.9(6), Pd(1)–H(1)–B(1) 110.2(12), Pd(1)–H(2)–B(1) 80.2(12), C(1)–Pd(1)–B(1) 165.62(8), P(1)-Pd(1)-P(2) 155.67(2).
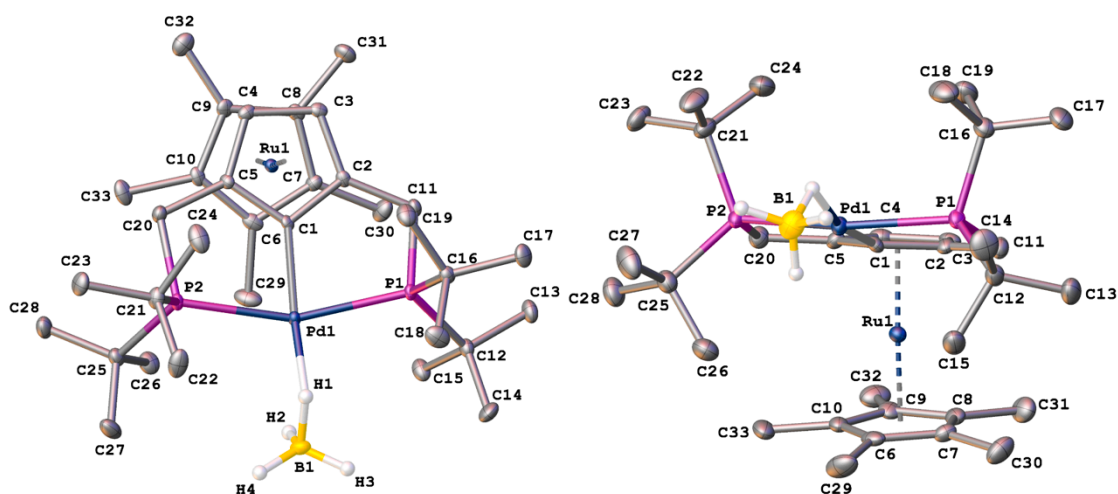

Figure 2. Two views of the compound **3b** in representation of atoms via thermal ellipsoids at 50% probability level. Selected bond lengths (Å) and angles (°): Pd(1)–C(1) 1.990(5), Pd(1)–P(1) 2.3409(13), Pd(1)–P(2) 2.3453(13), Pd(1)···B(1) 2.560(7), Pd(1)–H(1) 1.82(5), Pd(1)···H(2) 2.34(6); C(1)–Pd(1)–H(1) 166.8(18), Pd(1)–H(1)–B(1) 118(4), Pd(1)–H(2)–B(1) 90(3), C(1)–Pd(1)–B(1) 170.0(2), P(1)Pd(1)P(2) 158.87(5).

In complexes **3a** and **3b**, the Pd···B distance exceeds the sum of the covalent radii of Pd and B atoms (ca. 2.2 Å) being 2.531(2) and 2.560 (7) Å, respectively. For comparison, in complex **3c**, the Pd···B distance is 2.587(3) Å [36]. Obviously, a decrease in the Pd···B distance in the series of compounds **3** indicates an increase in the strength of the BH$_4$ bond with the palladium atom. For comparison, in the recently described monodentate and bidentate borohydride complexes supported by benzene based pincer ligands, the Pd···B distance varies in the range 2.42–2.47 Å [42,43]. It is interesting to note that the angle C(1)-Pd(1)-B(1) is 170.3(1)° in the complex Rc[PCP^{tBu}]Pd(BH$_4$) (**3c**) [36] and 170.0(2)° in Rc*[PCP^{tBu}]Pd(BH$_4$) (**3b**), while in Rc^F[PCP^{tBu}]Pd(BH$_4$) (**3a**) it is 165.62(8)°.

Presumably, the additional (relative to complexes **3b** and **3c**) deviation of 4.4–4.7° from linearity in **3a** is due to the greater steric pressure of the bulky axial *tert*-butyl groups at phosphorus atoms on the borohydride ligand. Indeed, the distance between the central carbon atoms C(16) and C(21) of the axial *tert*-butyl groups in complexes **3a** and **3b** is 5.573(3) and 5.759(6) Å, respectively. For comparison, the same distance in complex **3c** is 6.006(3) Å [36]. Thus, despite the bulky CF_3 group is in the remote position relative to $Pd(BH_4)$ fragment, it affects the overall geometry of this pincer complex: the decreased inclination of two Cp rings puts three methyl groups close to *tert*-butyls pushing both tBu_2P fragments above the plane of cyclometalated ring away from to the ruthenium atom. That, in turn, expels BH_4 moiety below the same plane decreasing the C(1)-Pd(1)-B(1) angle.

2.3. IR Spectra

Vibrational spectra are often used to determine the type of BH_4 group coordination to transition metal [39,44]. The IR spectra of complexes **3a** and **3b** are similar to the spectrum of the previously published $Rc[PCP^{tBu}]Pd(BH_4)$ (**3c**) complex (Figures S14–S17). In agreement with the crystallographic data, they indicate the presence of a secondary Pd⋯H interaction in addition to the primary Pd-H bond both in the crystalline state and in solution. In the spectra of solid samples of complexes **3a** and **3b**, the stretching vibration $\nu^{as}(B-H_{term})$ of the terminal B-H bonds is observed in the frequency range 2363–2388 cm^{-1} either as a split band (in case of **3a**) or as a band with a shoulder (**3b**). Probably, the splitting is associated with the isotopic effect of $^{10}B-H/^{11}B-H$ [39] vibrations. In the CH_2Cl_2 solution of complexes **3a** and **3b**, the same vibration appears as a non-split strong band at 2376 and 2372 cm^{-1}, respectively. Note that, in the series of complexes **3**, a shift of this band to a higher frequency region is observed (Table 1), which may indicate an increase in the contribution of the bidentate form of BH_4 coordination [39,44]. The stretching bands $\nu^{s}(B-H_{term})$ of moderate intensity are observed in the IR spectrum of solid samples **3a** and **3b** at 2296 and 2291 cm^{-1}, respectively. The stretching vibrations $\nu(B-H_{bridge})$ of a bridging hydrogen atom Pd-H-B in the spectra of complexes **3a**, **3b** appear as wide bands of moderate intensity at 2019 and 2025 cm^{-1} and a high-intensity band in the lower frequency region at 1838 and 1846 cm^{-1}, respectively. It should be noted that $\nu(B-H_{bridge})$ stretching vibrations in the low-frequency region at 1700-2000 cm^{-1} are rarely observed in the IR spectra of $M(\eta^1-BH_4)$ complexes, but as a rule always present in the spectra of $M(\eta^2-BH_4)$ complexes [44]. The bands of bending vibrations $\delta(BH)$ in the spectra of complexes **3a**, **3b** are observed at 1054 and 1060 cm^{-1}, respectively, that is in the frequency range characteristic rather for the η^1-bound BH_4 ligand [39,44].

Table 1. Selected FTIR data for complexes **3a**–**3c** (band positions in cm^{-1}).

	3a(KBr)	3b(KBr)	3c(KBr) [36]	3a(CH$_2$Cl$_2$)	3b(CH$_2$Cl$_2$)
$\nu^{as}(B-H_{term})$	2388, 2363	2374	2364	2376	2372
$\nu^{s}(B-H_{term})$	2296	2291	2292	2289	2287
$\nu_1(B-H_{bridge})$	2019	2025	1993	2019	2008
$\nu_2(B-H_{bridge})$	1838	1846	1840	1840	1841
$\delta(BH)$	1054	1060		1062	1062

3. Materials and Methods

3.1. General Considerations

All synthetic work was performed under a purified argon atmosphere using standard Schlenk techniques. The solvents were dried and degassed by standard methods under an argon atmosphere. Deuterated solvents were freshly distilled under argon prior to use. The starting compounds 1,3-bis(di-*tert*-butylphosphinomethyl)-1′-(trifluoromethyl)-2′,3′,4′,5′-(tetramethyl)-ruthenocene (**1**) [37] and {2,5-bis(di-*tert*-butylphosphinomethyl)-1′,2′,3′,4′,5′-(pentamethyl)-ruthenocen-1-yl}palladium chloride (**2b**) [17] were prepared by known procedures.

The ^{1}H, ^{19}F, ^{11}B{^{1}H} NMR spectra were recorded on a Bruker Avance 400 spectrometer. ^{1}H chemical shifts are reported in ppm downfield to TMS using the residual signals of the solvent (CDCl$_3$, δ 7.26; C$_6$D$_6$, δ 7.16) as the internal standard. The ^{19}F and ^{11}B{^{1}H} NMR spectra are given on the δ scale, the chemical shifts were measured relative to CFCl$_3$ and BF$_3$·Et$_2$O, respectively, as external standards. ^{31}P{^{1}H} NMR spectra were recorded on Bruker Avance 300, or Bruker Avance 400 spectrometers and are reported in ppm using 85% H$_3$PO$_4$ as external standard. ^{13}C{^{1}H} NMR spectra were recorded on a Bruker Avance 600 spectrometer with CDCl$_3$ (δ 77.16) or C$_6$D$_6$ (δ 128.06) as the internal reference. FTIR spectra were measured on Shimadzu IR Prestige 21 FTIR spectrometer. Elemental analysis was performed at the Laboratory of Microanalysis of INEOS RAS. Single crystals of **3a** and **3b** were obtained by slow crystallization from toluene/hexane mixture.

3.2. Crystallographic Data

Crystals of **3a** (C$_{33}$H$_{58}$BF$_3$P$_2$PdRu, M = 792.01) are monoclinic, space group P2$_1$/c, at 120 K: a = 18.5494(6), b = 12.0953(4), c = 15.8197(5) Å, β = 90.2560(10)°, V = 3549.3(2) Å^3, Z = 4 (Z' = 1), d$_{calc}$ = 1.482 g·cm^{-3}, μ(MoKα) = 10.59 cm^{-1}, F(000) = 1632. Crystals of **3b** (C$_{33}$H$_{61}$BP$_2$PdRu, M = 738.03) are orthorhombic, space group P2$_1$2$_1$2$_1$, at 120 K: a = 11.3765(5), b = 15.0316(6), c = 21.0022(9) Å, V = 3591.5(3) Å^3, Z = 4 (Z' = 1), d$_{calc}$ = 1.365 g·cm^{-3}, μ(MoKα) = 10.30 cm^{-1}, F(000) = 1536. Intensities of 72725 and 36743 reflections were measured with a Bruker APEX2 DUO CCD diffractometer [λ(MoKα) = 0.71073 Å, ω-scans, 2θ < 58°] for **3a** and **3b**, respectively; 9442 and 9578 independent reflections [R$_{int}$ 0.0522 and 0.0518] were used in a further refinement. Using Olex2 [45], the structures were solved with the ShelXT structure solution program [46] using Intrinsic Phasing and refined with the XL refinement package [47] using Least-Squares minimization. Hydrogen atoms of the BH groups were located from difference Fourier synthesis and refined freely in the isotropic approximation. Positions of all other atoms were calculated, and they were refined within the riding model. For **3a**, the refinement converged to wR2 = 0.0535 and GOF = 1.023 for all the independent reflections (R1 = 0.0235 was calculated against F for 8034 observed reflections with I > 2σ(I)). For **3b**, the refinement converged to wR2 = 0.0729 and GOF = 1.009 for all the independent reflections (R1 = 0.0394 was calculated against F for 8230 observed reflections with I>2σ(I)). CCDC 1993081 and 1993082 contain the supplementary crystallographic information for **3a** and **3b**, respectively. Crystal data and structure refinement parameters for **3a**, **3b** are summarized in Table S1.

3.3. Synthesis

3.3.1. Preparation of {2,5-Bis(di-tert-butylphosphinomethyl)-1'-(trifluoromethyl)-2',3',4',5'-(tetramethyl)ruthenocen-1-yl]palladium(II) chloride PdCl[{2,5-(^{t}Bu$_2$PCH$_2$)$_2$C$_5$H$_2$}Ru(C$_5$Me$_4$CF$_3$)] (**2a**)

PdCl$_2$(PhCN)$_2$ (270 mg, 0.703 mmol) was added to a suspension of bisphosphine **1** (470 mg, 0.700 mmol) in 2-methoxyethanol (20 mL). The mixture was refluxed with stirring for 3 h, then triethylamine (0.20 mL, 1.45 mmol) was rapidly added to the boiling solution using a syringe and the mixture was refluxed for additional 2 h. After cooling the resulting solution was diluted with dichloromethane (1:1) and filtered through celite. Then the solvents were removed in vacuo, and the residue was purified on an alumina column (eluent hexane- dichloromethane (2:1)). Recrystallization of the residue from ethanol gave pale-yellow solid of the product. Yield: 175 mg (31%). ^{1}H NMR (400.13 MHz, CDCl$_3$, 294 K): 1.33 (vt, 18H, J_{HP} = 13.1, C(CH$_3$)$_3$), 1.47 (vt, 18H, J_{HP} = 14.6, C(CH$_3$)$_3$), 1.77 (s, 6H, 3,4-C$_5$(C$\underline{H}_3$)$_2$(CH$_3$)$_2$CF$_3$), 1.89 (br. m, 6H, 2,5-C$_5$(CH$_3$)$_2$(C$\underline{H}_3$)$_2$CF$_3$), 2.45 (dvt, 2H, J_{HH} = 16.6, J_{HP} = 6.3, C$\underline{H}_A$H$_B$P), 2.51 (dvt, 2H, J_{HH} = 16.6, J_{HP} = 8.7, CH$_A$$\underline{H}_B$P), 4.22 (s, 2H, C$_5H_2$). ^{31}P{^{1}H} NMR (161.98 MHz, CDCl$_3$, 294 K): 82.07 (s, 2P). ^{19}F NMR (376.50 MHz, CDCl$_3$, 294 K): -52.74 (s, 3F, CF$_3$). ^{13}C{^{1}H} NMR (150.93 MHz, CDCl$_3$, 293 K): 10.61 (s, 2C, 3,4-C$_5$(C$\underline{H}_3$)$_2$(CH$_3$)$_2$CF$_3$), 11.23 (q, 2C, J_{CF} = 2.3, 2,5-C$_5$(CH$_3$)$_2$(C$\underline{H}_3$)$_2$CF$_3$), 22.68 (vt, 2C, J_{CP} = 19.5, CH$_2$), 29.58 (vt, 6C, J_{CP} = 5.7, C(C$\underline{H}_3$)$_3$), 29.75 (vt, 6C, J_{CP} = 7.3, C(C$\underline{H}_3$)$_3$), 34.36 (vt, 2C, J_{CP} = 13.7, $\underline{C}$(CH$_3$)$_3$), 35.79 (vt, 2C, J_{CP} = 11.2, $\underline{C}$(CH$_3$)$_3$), 71.48 (vt, 2C, J_{CP} = 16.5, 3,4-C$_5$H$_2$), 76.77 (q, 1C, J_{CF} = 35.5, $\underline{C}$-CF$_3$), 82.50 (s, 2C, $\underline{C}_5$(CH$_3$)$_4$CF$_3$), 87.43 (s, 2C,

$\underline{C}_5(CH_3)_4CF_3$), 97.26 (vt, 2C, J_{CP} = 29.3, 2,5-C_5H_2), 118.98 (s, 1C, 1-C_5H_2), 128.27 (q, 1C, J_{CF} = 270.0, CF_3). Anal. Calc. for $C_{33}H_{54}F_3ClP_2PdRu$ (Mr = 812.75): C, 48.76; H, 6.71; P, 7.62; Cl, 4.36%. Found: C, 48.54; H, 6.82; P, 7.49; Cl, 4.48%.

3.3.2. General Procedure for Preparation of Palladium Tetrahydroborate Complexes **3a** and **3b**

NaBH$_4$ (100 mg, 2.63 mmol) was added to a solution of complexes **2a** or **2b** (110–120 mg) in 20 mL of ethanol-benzene (10:1) mixture at room temperature. The mixture was refluxed for 8 h, adding 50 mg (1.32 mmol) of NaBH$_4$ to the mixture every hour. The reaction mixture was then cooled and evaporated in vacuo to a minimum volume. Distilled water (20 mL) was added to the residue, the resulting suspension was stirred at room temperature for 1 h. The reaction mass was extracted (4 × 10 mL) with hexane-benzene (3:1). The solvents were evaporated in vacuo. Recrystallization of the residue from toluene-hexane (1:1) mixture gave solid products (**3a** or **3b**), which were additionally dried in vacuo at room temperature.

Preparation of {2,5-Bis(di-tert-butylphosphinomethyl)-1′-(trifluoromethyl)-2′,3′,4′,5′-(tetramethyl)-ruthenocen-1-yl]palladium(II) tetrahydroborate
Pd(BH$_4$)[{2,5-($^tBu_2PCH_2)_2C_5H_2$}Ru($C_5Me_4CF_3$)] (**3a**)

Complex **3a** obtained from 118 mg (0.145 mol) of complex **2a** as a yellow powder. Yield: 104 mg (90%). ^{1}H NMR (400.13 MHz, C_6D_6, 293 K): 0.13 (br. m, 4H, BH$_4$), 1.15 (vt, 18H, J_{HP} = 13.4, C(CH$_3$)$_3$), 1.40 (vt, 18H, J_{HP} = 14.4, C(CH$_3$)$_3$), 1.66 (s, 6H, 3,4-C_5(C$\underline{H}_3$)$_2$(CH$_3$)$_2$CF$_3$), 1.95 (br. m, 6H, 2,5-C_5(CH$_3$)$_2$(C$\underline{H}_3$)$_2$CF$_3$), 2.08 (dvt, 2H, J_{HH} = 16.6, J_{HP} = 9.2, C$\underline{H}_A$H$_B$P), 2.32 (dvt, 2H, J_{HH} = 16.6, J_{HP} = 5.9, CH$_A$$\underline{H}_B$P), 4.25 (s, 2H, C_5H_2). ^{11}B{^{1}H} (128.38 MHz, C_6D_6, 295 K): −34.54 (br.s, 1B, BH$_4$). ^{31}P{^{1}H} NMR (121.49 MHz, C_6D_6, 293 K): 87.44 (s, 2P). ^{19}F NMR (376.50 MHz, C_6D_6, 295 K): −52.05 (s, 3F, CF$_3$). ^{13}C{^{1}H} NMR (150.93 MHz, C_6D_6, 294 K): 10.57 (s, 2C, 3,4-C_5(C$\underline{H}_3$)$_2$(CH$_3$)$_2$CF$_3$), 11.44 (br. m, 2C, 2,5-C_5(CH$_3$)$_2$(C$\underline{H}_3$)$_2$CF$_3$), 23.36 (vt, 2C, J_{CP} = 20.3, CH$_2$), 29.55 (vt, 6C, J_{CP} = 7.1, C(C$\underline{H}_3$)$_3$), 29.63 (vt, 6C, J_{CP} = 6.0, C(C$\underline{H}_3$)$_3$), 34.70 (vt, 2C, J_{CP} = 14.4, $\underline{C}$(CH$_3$)$_3$), 35.27 (vt, 2C, J_{CP} = 11.4, $\underline{C}$(CH$_3$)$_3$), 71.43 (vt, 2C, J_{CP} = 16.5, 3,4-C_5H_2), 77.03 (q, 1C, J_{CF} = 35.3, $\underline{C}$-CF$_3$), 82.65 (s, 2C, $\underline{C}_5$(CH$_3$)$_4$CF$_3$), 87.45 (s, 2C, $\underline{C}_5$(CH$_3$)$_4$CF$_3$), 97.82 (vt, 2C, J_{CP} = 28.8, 2,5-C_5H_2), 121. 77 (s, 1C, 1-C_5H_2), 129.22 (q, 1C, J_{CF} = 269.9, CF$_3$). FTIR (KBr pellet, ν in cm^{-1}): 2388 (s, B-H$_t$), 2363 (s, B-H$_t$), 2296 (s, B-H$_t$), 2019 (br. w, B-H$_{br}$-Pd), 1838 (br. s, B-H$_{br}$-Pd), 1054 (s, δ$_{BH3}$). FTIR (CH$_2$Cl$_2$, ν in cm^{-1}): 2376 (s(sh), B-H$_t$), 2289 (s, B-H$_t$), 2019 (br. w, B-H$_{br}$-Pd), 1840 (s, B-H$_{br}$-Pd), 1062 (s, δ$_{BH3}$). Anal. Calc. for $C_{33}H_{58}BF_3P_2PdRu$ (M$_r$ = 792.06): C, 50.04; H, 7.38%. Found: C, 50.29; H, 7.48%.

Preparation of
{2,5-Bis(di-tert-butylphosphinomethyl)-1′,2′,3′,4′,5′-(pentamethyl)ruthenocen-1-yl]palladium(II) tetrahydroborate Pd(BH$_4$)[{2,5-($^tBu_2PCH_2)_2C_5H_2$}Ru(C_5Me_5)] (**3b**)

Complex **3b** obtained from 114 mg (0.150 mol) of complex **2b** as a yellow powder. Yield: 103 mg (93%). ^{1}H NMR (400.13 MHz, C_6D_6, 295 K): 0.21 (br.m, 4H, BH$_4$), 1.20 (vt, 18H, J_{HP} = 13.0, C(CH$_3$)$_3$), 1.47 (vt, 18H, J_{HP} = 14.3, C(CH$_3$)$_3$), 1.84 (s, 15H, C_5(CH$_3$)$_5$), 2.15 (dvt, 2H, J_{HH} = 16.5, J_{HP} = 9.1, C$\underline{H}_A$H$_B$P), 2.38 (dvt, 2H, J_{HH} = 16.5, J_{HP} = 5.9, CH$_A$$\underline{H}_B$P), 3.95 (s, 2H, C_5H_2). ^{11}B{^{1}H} (128.38 MHz, C_6D_6, 295 K): −34.73 (br.s, 1B, BH$_4$). ^{31}P{^{1}H} NMR (161.98 MHz, C_6D_6, 295 K): 87.07 (s, 2P). ^{13}C{^{1}H} NMR (150.93 MHz, C_6D_6, 293 K): 11.49 (s, 5C, C_5(C$\underline{H}_3$)$_5$), 23.42 (vt, 2C, J_{CP} = 20.4, CH$_2$), 29.71 (m, 12C, C(C$\underline{H}_3$)$_3$), 34.67 (vt, 2C, J_{CP} = 14.3, $\underline{C}$(CH$_3$)$_3$), 35.22 (vt, 2C, J_{CP} = 11.1, $\underline{C}$(CH$_3$)$_3$), 71.43 (vt, 2C, J_{CP} = 16.9, 3,4-C_5H_2), 83.99 (s, 5C, $\underline{C}_5$(CH$_3$)$_5$), 95.84 (vt, 2C, J_{CP} = 29.1, 2,5-C_5H_2), 120. 55 (s, 1C, 1-C_5H_2). FTIR (KBr pellet, ν in cm^{-1}): 2374 (s(sh), B-H$_t$), 2291 (s, B-H$_t$), 2025 (br.w, B-H$_{br}$-Pd), 1851 (s, B-H$_{br}$-Pd), 1060 (s, δ$_{BH3}$). FTIR (CH$_2$Cl$_2$, ν in cm^{-1}): 2372 (s(sh), B-H$_t$), 2287 (s, B-H$_t$), 2008 (br. w, B-H$_{br}$-Pd), 1841 (s, B-H$_{br}$-Pd), 1062 (s, δ$_{BH3}$). Anal. Calc. for $C_{33}H_{61}BP_2PdRu$ (M$_r$ = 738.09): C, 53.70; H, 8.33; P, 8.39%. Found: C, 53.84; H, 8.38; P, 8.13%.

4. Conclusions

Thus, our work demonstrated that the introduction of the bulky $C_5Me_4CF_3$ (Cp^F) and C_5Me_5 (Cp^*) ligands in the sandwich scaffold of the ruthenocene-based PCP^{tBu} pincer palladium complexes does not preclude the formation of the corresponding palladium tetrahydroborate pincer complexes. The two novel sterically loaded pincer palladium tetrahydroborates $Rc^F[PCP^{tBu}]Pd(BH_4)$ (**3a**) and $Rc^*[PCP^{tBu}]Pd(BH_4)$ (**3b**) were synthesized and fully characterized by X-ray, NMR, and FTIR techniques. The X-ray diffraction study of **3a** and **3b** revealed that an increase of the steric bulk of non-metalated cyclopentadienyl ring in **3a** and **3b** relative to non-substituted $Rc[PCP^{tBu}]Pd(BH_4)$ analogue (**3c**) pushes palladium atom from the middle plane of the metalated Cp ring in the direction opposite to the ruthenium atom. This displacement increases in the order **3c** < **3b** < **3a** following the order of the Cp-ring steric volume increase. The analysis of both X-ray and IR data suggests that BH_4 ligand in both palladium tetrahydroborates **3a** and **3b** has the mixed coordination mode $\eta^{1,2}$ similar to that in **3c** in which the primary Pd-H contact of 1.82–1.87Å is accompanied by the secondary interaction Pd···H of 2.34–2.54Å. Pd···B distances decrease in the order: $Rc[PCP^{tBu}]Pd(BH_4)$ > $Rc^*[PCP^{tBu}]Pd(BH_4)$ > $Rc^F[PCP^{tBu}]Pd(BH_4)$ that suggests the increase in the strength of the BH_4 bond with the palladium atom that appears to be affected by both steric and electronic properties of the ruthenocene moiety.

Supplementary Materials: The following are available online, Table S1: Crystal data and structure refinement parameters for **3a**, **3b**. Figure S1: ^1H NMR spectrum (400.13 MHz) of **2a** in $CDCl_3$. Figure S2: $^{31}P\{^1H\}$ NMR spectrum (161.98 MHz) of **2a** in $CDCl_3$. Figure S3: ^{19}F NMR spectrum (376.50 MHz) of **2a** in $CDCl_3$. Figure S4: $^{13}C\{^1H\}$ NMR spectrum (150.93 MHz) of **2a** in $CDCl_3$. Figure S5: ^1H NMR spectrum (400.13 MHz) of **3a** in C_6D_6. Figure S6: $^{11}B\{^1H\}$ NMR spectrum (128.38 MHz) of **3a** in C_6D_6. Figure S7: $^{31}P\{^1H\}$ NMR spectrum (121.49 MHz) of **3a** in C_6D_6. Figure S8: ^{19}F NMR spectrum (376.50 MHz) of **3a** in C_6D_6. Figure S9: $^{13}C\{^1H\}$ NMR spectrum (150.93 MHz) of **3a** in C_6D_6. Figure S10: ^1H NMR spectrum (400.13 MHz) of **3b** in C_6D_6. Figure S11: $^{11}B\{^1H\}$ NMR spectrum (128.38 MHz) of **3b** in C_6D_6. Figure S12: $^{31}P\{^1H\}$ NMR spectrum (161.98 MHz) of **3b** in C_6D_6. Figure S13: $^{13}C\{^1H\}$ NMR spectrum (150.93 MHz) of **3b** in C_6D_6. Figure S14: FTIR spectra of **3a** in KBr pellet. Figure S15: FTIR spectra of **3b** in KBr pellet. Figure S16: FTIR spectra of **3a** in the CH_2Cl_2 solution. Figure S17: FTIR spectra of **3b** in the CH_2Cl_2 solution.

Author Contributions: Investigation S.V.S., E.S.O., Y.V.N., O.A.F., I.G.B.; Writing—Original Draft Preparation, S.V.S. and O.A.F.; Writing—Review and Editing, N.V.B.; Supervision, E.S.S. All authors have read and agreed to the published version of the manuscript.

Conflicts of Interest: The authors declare no conflict of interest.

References

1. Moulton, C.J.; Shaw, B.L. Transition metal-carbon bonds. Part XLII. Complexes of nickel, palladium, platinum, rhodium and iridium with the tridentate ligand 2,6-bis[(di-t-butylphosphino)methyl]phenyl. *J. Chem. Soc. Dalton Trans.* **1976**, 1020–1024. [CrossRef]
2. van Koten, G.; Milstein, D. *Organometallic Pincer Chemistry*; Top. Organomet. Chem.; Springer: Berlin/Heidelberg, Germany, 2013; pp. 1–356.
3. van Koten, G.; Gossage, R.A. *The Privileged Pincer-Metal Platform: Coordination Chemistry and Applications*; Top. Organomet. Chem.; Springer: Heidelberg, Germany, 2016; pp. 1–374.
4. Morales-Morales, D. *Pincer Compounds*; Elsevier BV: Amsterdam, The Netherlands, 2018; pp. 1–450.
5. Peris, E.V.; Crabtree, R.H. Key factors in pincer ligand design. *Chem. Soc. Rev.* **2018**, *47*, 1959–1968. [CrossRef] [PubMed]
6. Polukeev, A.V.; Wendt, O.F. Iridium complexes with aliphatic, non-innocent pincer ligands. *J. Organomet. Chem.* **2018**, *867*, 33–50. [CrossRef]
7. Asay, M.; Morales-Morales, D. Non-symmetric pincer ligands: Complexes and applications in catalysis. *Dalton Trans.* **2015**, *44*, 17432–17447. [CrossRef]

8. Choi, J.; MacArthur, A.H.R.; Brookhart, M.; Goldman, A. Dehydrogenation and Related Reactions Catalyzed by Iridium Pincer Complexes. *Chem. Rev.* **2011**, *111*, 1761–1779. [CrossRef]

9. Selander, N.; Szabó, K.J. Catalysis by Palladium Pincer Complexes. *Chem. Rev.* **2010**, *111*, 2048–2076. [CrossRef]

10. Leis, W.; Mayer, H.; Kaska, W. Cycloheptatrienyl, alkyl and aryl PCP-pincer complexes: Ligand backbone effects and metal reactivity. *Co-ord. Chem. Rev.* **2008**, *252*, 1787–1797. [CrossRef]

11. Van Der Boom, M.E.; Milstein, D. Cyclometalated Phosphine-Based Pincer Complexes: Mechanistic Insight in Catalysis, Coordination, and Bond Activation. *Chem. Rev.* **2003**, *103*, 1759–1792. [CrossRef]

12. Albrecht, M.; Van Koten, G. Platinum Group Organometallics Based on "Pincer" Complexes: Sensors, Switches, and Catalysts. *Angew. Chem. Int. Ed.* **2001**, *40*, 3750–3781. [CrossRef]

13. Koridze, A.A.; Sheloumov, A.M.; Kuklin, S.A.; Lagunova, V.Y.; Petukhova, I.I.; Dolgushin, F.M.; Ezernitskaya, M.G.; Petrovskii, P.V.; Macharashvili, A.A.; Chedia, R.V. PCP pincer ligands based on metallocenes. Crystal structure of the rhodium complex *cis*-RhCl$_2$(CO)[{2,5-(Pr^i$_2$PCH$_2$)$_2$C$_5$H$_2$}Fe(C$_5$H$_5$)]. *Russ. Chem. Bull.* **2002**, *51*, 1077–1078. [CrossRef]

14. Farrington, E.J.; Viviente, E.M.; Williams, B.S.; Van Koten, G.; Brown, J.M. Synthesis and reactivity of a ferrocene-derived PCP-pincer ligand. *Chem. Commun.* **2002**, 308–309. [CrossRef] [PubMed]

15. Koridze, A.A.; Kuklin, S.A.; Sheloumov, A.M.; Dolgushin, F.M.; Lagunova, V.Y.; Petukhova, I.I.; Ezernitskaya, M.G.; Peregudov, A.S.; Petrovskii, P.V.; Vorontsov, E.V.; et al. Ferrocene-Based Pincer Complexes of Palladium: Synthesis, Structures, and Spectroscopic and Electrochemical Properties. *Organometallics* **2004**, *23*, 4585–4593. [CrossRef]

16. Kuklin, S.A.; Sheloumov, A.M.; Dolgushin, F.M.; Ezernitskaya, M.G.; Peregudov, A.S.; Petrovskii, P.V.; Koridze, A.A. Highly Active Iridium Catalysts for Alkane Dehydrogenation. Synthesis and Properties of Iridium Bis(phosphine) Pincer Complexes Based on Ferrocene and Ruthenocene. *Organometallics* **2006**, *25*, 5466–5476. [CrossRef]

17. Kuklin, S.A.; Dolgushin, F.M.; Petrovskii, P.V.; Koridze, A.A. Synthesis and comparative X-ray diffraction study of first ruthenocene-based pincer palladium complexes, PdCl[{2,5-(Bu^t $_2$PCH$_2$)$_2$C$_5$H$_2$}Ru(Cp')] (Cp' = C$_5$H$_5$ or C$_5$Me$_5$). *Russ. Chem. Bull.* **2006**, *55*, 1950–1955. [CrossRef]

18. Sheloumov, A.M.; Dolgushin, F.M.; Kondrashov, M.V.; Petrovskii, P.V.; Barbakadze, K.A.; Lekashvili, O.I.; Koridze, A.A. Ruthenium complexes with ferrocene-based P,C,P pincer ligand. *Russ. Chem. Bull.* **2007**, *56*, 1757–1764. [CrossRef]

19. Sheloumov, A.M.; Tundo, P.; Dolgushin, F.M.; Koridze, A.A. Suzuki Aryl Coupling Catalysed by Palladium Bis(phosphane) Pincer Complexes Based on Ferrocene; X-ray Structure Determination of {PdCl[{2,5-(*t*Bu$_2$PCH$_2$)$_2$C$_5$H$_2$}Fe(C$_5$H$_5$)]}OTf. *Eur. J. Inorg. Chem.* **2008**, 572–576. [CrossRef]

20. Safronov, S.V.; Sheloumov, A.M.; Kreindlin, A.Z.; Kamyshova, A.A.; Dolgushin, F.M.; Smol'yakov, A.F.; Petrovskii, P.V.; Ezernitskaya, M.G.; Koridze, A.A. P,C,P-Pincer complexes of ruthenium based on ruthenocene and pentamethylruthenocene. *Russ. Chem. Bull.* **2010**, *59*, 1740–1744. [CrossRef]

21. Koridze, A.A.; Polezhaev, A.V.; Safronov, S.V.; Sheloumov, A.M.; Dolgushin, F.M.; Ezernitskaya, M.G.; Lokshin, B.V.; Petrovskii, P.V.; Peregudov, A.S. Cationic Ruthenium Hydrido–Carbonyls Derived from Metallocene-Based Pincers: Unusual Rearrangements and H2Evolution with Formation of Cationic Ruthenium Metallocenylidenes. *Organometallics* **2010**, *29*, 4360–4368. [CrossRef]

22. Polukeev, A.V.; Kuklin, S.A.; Petrovskii, P.V.; Peregudova, S.M.; Smol'yakov, A.F.; Dolgushin, F.M.; Koridze, A.A. Synthesis and characterization of fluorophenylpalladium pincer complexes: Electronic properties of some pincer ligands evaluated by multinuclear NMR spectroscopy and electrochemical studies. *Dalton Trans.* **2011**, *40*, 7201–7209. [CrossRef]

23. Bonnet, S.; Lutz, M.; Spek, A.L.; Van Koten, G.; Klein Gebbink, R.J.M. η^6-Coordination of a Ruthenium(II) Organometallic Fragment to the Arene Ring of N,C,N-Pincer Metal Complexes. *Organometallics* **2008**, *27*, 159–162. [CrossRef]

24. Bonnet, S.; Van Lenthe, J.H.; Siegler, M.A.; Spek, A.L.; Van Koten, G.; Klein Gebbink, R.J.M. Bimetallic η^6,η^1 NCN-Pincer Ruthenium Palladium Complexes with η^6-RuCp Coordination: Synthesis, X-ray Structures, and Catalytic Properties⊥. *Organometallics* **2009**, *28*, 2325–2333. [CrossRef]

25. Bonnet, S.; Li, J.; Siegler, M.A.; Von Chrzanowski, L.S.; Spek, A.L.; Van Koten, G.; Klein Gebbink, R.J.M. Synthesis and Resolution of Planar-Chiral Ruthenium-Palladium Complexes with ECE' Pincer Ligands. *Chem.-A Eur. J.* **2009**, *15*, 3340–3343. [CrossRef] [PubMed]

26. Bonnet, S.; Lutz, M.; Spek, A.L.; Van Koten, G.; Klein Gebbink, R.J.M. Bimetallic η^6,η^1 SCS- and PCP-Pincer Ruthenium Palladium Complexes: Synthesis, Structure, and Catalytic Activity. *Organometallics* **2010**, *29*, 1157–1167. [CrossRef]

27. Walter, M.D.; White, P.S. [Cp'FeI]$_2$ as convenient entry into iron-modified pincer complexes: Bimetallic η^6,κ^1-POCOP-pincer iron iridium compounds. *New J. Chem.* **2011**, *35*, 1842–1854. [CrossRef]

28. Espinosa-Jalapa, N.Á.; Hernández-Ortega, S.; Morales-Morales, D.; Le Lagadec, R. Facile synthesis of heterobimetallic compounds from the cyclopentadienyl-ruthenium moiety and group 10 POCOP pincer complexes. *J. Organomet. Chem.* **2012**, *716*, 103–109. [CrossRef]

29. Espinosa-Jalapa, N.Á.; Hernández-Ortega, S.; Le Goff, X.; Morales-Morales, D.; Djukic, J.-P.; Le Lagadec, R. Coordination of 12-Electron Organometallic Fragments to the Arene Ring of Nonsymmetric Group 10 POCOP Pincer Complexes. *Organometallics* **2013**, *32*, 2661–2673. [CrossRef]

30. Espinosa-Jalapa, N.A.; Ramires, M.A.R.; Toscano, R.A.; Djukic, J.-P.; Le Lagadec, R. Preparative resolution of stable enantio-enriched POCOP-based planar chiral pincer complexes. *J. Organomet. Chem.* **2017**, *845*, 125–134. [CrossRef]

31. Eberhardt, N.A.; Guan, H. Nickel Hydride Complexes. *Chem. Rev.* **2016**, *116*, 8373–8426. [CrossRef]

32. Gassman, P.G.; Mickelson, J.W.; Sowa, J.R. 1,2,3,4-Tetramethyl-5-(trifluoromethyl)cyclopentadienide: A unique ligand with the steric properties of pentamethylcyclopentadienide and the electronic properties of cyclopentadienide. *J. Am. Chem. Soc.* **1992**, *114*, 6942–6944. [CrossRef]

33. Gassman, P.G.; Sowa, J.R.; Hill, M.G.; Mann, K.R. Electrochemical Studies of Organometallic Complexes with Tetra-*n*-butylammonium Tetrakis [3,5-bis(trifluoromethyl)phenyl]borate as the Electrolyte. X-ray Crystal Structure of [C$_5$(CF$_3$)Me$_4$Fe(C$_5$H$_5$)]. *Organometallics* **1995**, *14*, 4879–4885. [CrossRef]

34. Gusev, O.V; A Ievlev, M.; A Peganova, T.; Peterleitner, M.G.; Petrovskii, P.V.; Oprunenko, Y.F.; Ustynyuk, N.A. Synthesis and reduction of trifluoromethyl-substituted arenecyclopentadienylruthenium sandwiches [Ru(η^5-C$_5$Me$_4$CF$_3$)(η^6-C$_6$R$_6$)]+ (R=H, Me) and [Ru(η^5-C$_5$Me$_5$)(η^6-C$_6$H$_5$CF$_3$)]+. *J. Organomet. Chem.* **1998**, *551*, 93–100. [CrossRef]

35. Safronov, S.V.; Sheloumov, A.M.; Petrovskii, P.V.; Ezernitskaya, M.G.; Koridze, A.A. (1,3-Diformylindenyl)cyclopentadienyl ruthenium derivatives. *Russ. Chem. Bull.* **2012**, *61*, 2065–2069. [CrossRef]

36. Safronov, S.V.; Gutsul, E.I.; Golub, I.E.; Dolgushin, F.M.; Nelubina, Y.V.; Filippov, O.A.; Epstein, L.M.; Peregudov, A.S.; Belkova, N.V.; Shubina, E.S.; et al. Synthesis, structural properties and reactivity of ruthenocene-based pincer Pd(ii) tetrahydroborate. *Dalton Trans.* **2019**, *48*, 12720–12729. [CrossRef] [PubMed]

37. Safronov, S.V.; Koridze, A.A. New ruthenocene-based ruthenium pincer complex bearing the C$_5$Me$_4$CF$_3$ ligand. *Russ. Chem. Bull.* **2018**, *67*, 1247–1250. [CrossRef]

38. Adhikary, A.; Schwartz, J.R.; Meadows, L.M.; Krause, J.A.; Guan, H. Interaction of alkynes with palladium POCOP-pincer hydride complexes and its unexpected relation to palladium-catalyzed hydrogenation of alkynes. *Inorg. Chem. Front.* **2014**, *1*, 71–82. [CrossRef]

39. Marks, T.J.; Kolb, J.R. Covalent transition metal, lanthanide, and actinide tetrahydroborate complexes. *Chem. Rev.* **1977**, *77*, 263–293. [CrossRef]

40. Johansson, R.; Wendt, O.F. Synthesis and Reactivity of (PCP) Palladium Hydroxy Carbonyl and Related Complexes toward CO$_2$ and Phenylacetylene. *Organometallics* **2007**, *26*, 2426–2430. [CrossRef]

41. Suh, H.-W.; Schmeier, T.J.; Hazari, N.; Kemp, R.A.; Takase, M.K. Experimental and Computational Studies of the Reaction of Carbon Dioxide with Pincer-Supported Nickel and Palladium Hydrides. *Organometallics* **2012**, *31*, 8225–8236. [CrossRef]

42. Zhang, J.; Ding, Y.; Ma, Q.-Q.; Cao, B.; Chang, J.; Li, S.; Chen, X. Reactions of POCOP pincer palladium benzylthiolate complexes with BH$_3$·THF: Isolation and characterization of unstable POCOP-Pd(η^1-HBH$_3$) complexes. *J. Organomet. Chem.* **2019**, *882*, 50–57. [CrossRef]

43. Ding, Y.; Ma, Q.-Q.; Kang, J.; Zhang, J.; Li, S.; Chen, X. Palladium(ii) complexes supported by PBP and POCOP pincer ligands: A comparison of their structure, properties and catalytic activity. *Dalton Trans.* **2019**, *48*, 17633–17643. [CrossRef]

44. Makhaev, V.D. Structural and dynamic properties of tetrahydroborate complexes. *Russ. Chem. Rev.* **2000**, *69*, 727–746. [CrossRef]

45. Dolomanov, O.; Bourhis, L.J.; Gildea, R.; Howard, J.A.K.; Puschmann, H. OLEX2: A complete structure solution, refinement and analysis program. *J. Appl. Crystallogr.* **2009**, *42*, 339–341. [CrossRef]

46. Sheldrick, G.M. SHELXT-integrated space-group and crystal-structure determination. *Acta Cryst.* **2015**, *A71*, 3–8. [CrossRef] [PubMed]

47. Sheldrick, G.M. A short history of SHELX. *Acta Cryst.* **2008**, *A64*, 112–122. [CrossRef] [PubMed]

Sample Availability: Not available.